Colloid Polym Sci (2004) 282: 773–781
DOI 10.1007/s00396-004-1091-6

ORIGINAL CONTRIBUTION

Günter Lieser
Gerhard Wegner
Jason A. Smith
Kenneth B. Wagener

Morphology and packing behavior of model ethylene/propylene copolymers with precise methyl branch placement

Received: 22 January 2004
Accepted: 3 March 2004
Published online: 29 April 2004

Dedicated to Professor Erhard W. Fischer on the occasion of his 75th birthday.

G. Lieser (✉) · G. Wegner
Max Planck Institut für Polymerforschung,
Ackermannweg 10, 55128 Mainz,
Germany
E-mail: lieser@mpip-mainz.mpg.de
Tel.: +49-6131-379136
Fax: +49-6131-379100

J. A. Smith · K. B. Wagener
The George and Josephine Butler
Polymer Research Laboratory,
Department of Chemistry,
University of Florida,
Gainesville, Florida 32611-7200, USA

Abstract The packing behavior of ethylene/propylene (E/P) copolymers with precise methyl group placement on every 15th and 21st chain carbon atom (denominated **HP15** and **HP21**) was investigated. Lamellar morphology with lamella thicknesses by far exceeding the distance between side groups gives strong evidence that the crystals contain pendant methyl groups as defects. The packing of chains in the lattice requires that adjacent E/P copolymer molecules stagger thereby forming a triclinic lattice with a hexagonal subcell of methylene groups. Defects inside the crystalline region are concentrated in planes oblique to the chain stems. The relationship between subcell and unit cell seems to be a function of the thermal history of the copolymer involving transient states. The atactic structure leads to conformationally disordered crystals (Wunderlich's CONDIS crystals) and enforces deviations from an *all-trans* stem conformation. These deviations shorten the chains and are stronger for **HP15** than for **HP21**, a fact that has been supported by Raman spectroscopy performed on recrystallized samples of both materials. In fact, a Raman signature band found at 1,084 cm^{-1} for only **HP15** indicates the presence of disordered chain conformations adjacent to singularities.

Introduction

Copolymerization of ethylene with various *alpha*-olefins (1-alkenes) gives a class of polyethylenes (PEs) known as linear low-density polyethylene (LLDPE). To date, structural studies concerning branching in LLDPE have focused on how the type and content of branches influence the molecular-level structure [1, 2, 3, 4, 5, 6, 7, 8, 9, 10, 11, 12, 13, 14, 15, 16], whereas the topic of how the branch sequence length distribution affects the final morphology and thereby physical properties has not been fully investigated [17, 18, 19]. The lack of relevant experimental data is largely due to synthetic limitations to precisely create and place the branches. In addition, the chain propagation chemistry is likely to introduce further defects by backbiting, chain transfer, chain walking, and similar effects. As a direct consequence of these side reactions as well as differences in reactivity between ethylene and a given 1-alkene, the placement of the branch is a random event. To address the question of what the true impact a given branch has on the final material's response, a synthetic method was needed to create a series of linear low-density polyethylenes in which branch placement occurs within a precise sequence length of the methylene groups, thereby, creating a completely homogeneous microstructure.

Recently, a method was reported that eliminates chain-transfer reactions as well as the random nature of branching in ethylene/α-olefin materials by using the clean polycondensation chemistry offered by acyclic diene metathesis (ADMET) [20]. ADMET creates ethylene/α-olefin systems with both a homogeneous composition distribution of branches and well-controlled polydispersity of typically around 2.0. This

presents an opportunity to investigate the physical properties of ethylene/α-olefin copolymers with narrow composition distribution, attributes that lend well to the modeling of the material responses for classes of LLDPE made by metallocene catalysis. Therefore, this chemistry facilitates studies of the role of short-chain branching (SCB) and short-chain branching distribution (SCBD) for the ultimate material's response of ethylene/α-olefin systems. Most recently, a series of five ethylene/propylene (E/P) copolymers were reported in which a methyl branch was precisely placed on each and every 9th, 11th, 15th, 19th, and 21st carbon along the backbone of PE (**HP9**, **HP11**, **HP15**, **HP19**, and **HP21**). Here, **HP** is an acronym for "hydrogenated polymer" and the numbers refer to the n-th carbon on which the branch is precisely placed [20]. A general retrosynthetic scheme for this new class of E/P copolymers is shown in Scheme 1.

For two of these materials, **HP15** and **HP21**, we describe herein X-ray and electron diffraction investigations to elucidate morphology and packing behavior. The most important aim is to find out how the precise placement of the methyl branches influences the chain packing in the crystalline state. Does the material allow for methyl branch incorporation both inside the crystalline lamellae and into the amorphous region, or does the precise branch placement lead to limitations in crystallite size along the chain trajectory? In the literature, the number of methyl groups per 1,000 methylene groups is used as an appropriate parameter to characterize the amount of branching. In comparison to previously investigated LLDPEs the amount of methyl branches is rather high. It amounts to 67 methyl groups per 1,000 C atoms for **HP15** and 48 per 1,000 for **HP21**.

Experimental

Copolymers and preparation

The synthesis of the ADMET copolymers was recently published elsewhere [20]. The number average molecular weights $(\overline{M_n})$ of the samples used in this work were 17.1 kg mol^{-1} for **HP15** and 20.2 kg mol^{-1} for **HP21** (relative to polystyrene standards) that have average contour chain lengths of 149 nm and 175 nm. Thin samples for electron microscopy and diffraction were prepared from dilute solutions of the copolymers in chloroform that were spread onto a water surface and subsequently transferred to carbon-coated copper grids. Prior to insertion into the electron microscope, the thin films were melted and recrystallized. The copolymers spread onto a water surface adopted homeopolar orientation. For E/P copolymer, crystallization from chloroform or tetrachloroethylene solution was used. The latter solvent was preferred for its lower vapor pressure and because its density exceeds the density of crystalline PE. This prevented the growing crystals coming into contact too early with the glass substrate onto which the solution was allowed to evaporate.

Wide-angle X-ray diffraction (WAXD)

X-ray investigations were performed with solid samples of powder texture. The samples were recrystallized from the melt in glass capillaries. Attempts to orient the polymers by drawing from the melt were unsuccessful. Threads could be formed but their texture remained powder-like. WAXD was performed using a double-radius Debye–Scherrer or a Kiessig camera with a fixed camera length of 100 mm. Both cameras used Ni-filtered Cu K_α as radiation source. Diffraction patterns were recorded at room temperature on Kodak Direct Exposure X-ray film and developed in an Agfa G150 developer.

Small-angle X-ray scattering (SAXS)

For SAXS a Kiessig camera with pinhole collimation and photographic registration was used at 200 and 400 mm sample–film distances.

Electron microscopy and diffraction

For transmission electron microscopic (TEM) inspection thin samples were shadowed by platinum and carbon. Subsequently a carbon supporting film was evaporated. Sample and carbon film were floated off the glass onto a water surface, from where they were transferred to copper grids. For electron diffraction the Pt/C shadowing was omitted. Owing to the high irradiation sensitivity most of the electron diffraction work was performed at a temperature of −130°C to reduce irradiation damage. The following instruments were used: a LEO TEM 912 operated at 120 kV for electron diffraction and a LEO TEM 902 operated at 80 kV for imaging. The electron energy-loss spectrometers

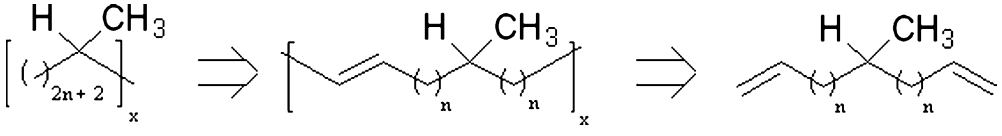

Scheme 1 Retrosynthetic methodology to produce E/P model copolymers via ADMET

integrated in the column of both instruments were only used to suppress inelastically scattered electrons. Areas from which electron diffraction patterns were recorded had diameters of 2.7 μm or 1.5 μm. Diffraction patterns were calibrated by means of an evaporated TlCl film. For photographic registration Ilford PAN F 35-mm film was used.

Raman spectroscopy

Raman spectra were obtained at the resolution of 2 cm^{-1} by a Dilor XY-800 spectrometer with a CCD detector (Type CCD05, Wright Instruments) with various laser sources.

Results

Morphology and lamella thickness of **HP15** and **HP21**

Solution-grown crystals of the ethylene/propylene (E/P) copolymers with precise methyl branching do not exhibit the pattern of uniform, lozenge-shaped platelets with some overgrowth as normally observed for linear PE [6, 21, 22, 23, 24]. Rather platelets of irregular shape are observed which grow—as is also observed for linear PE—round a screw dislocation if obtained from a solution in tetrachloroethylene. The growth planes are not straight as, for example, the (110) planes in the lamellae of linear polyethylene. A typical morphology exhibiting a growth spiral is displayed in Fig. 1. Since the ADMET E/P copolymers are soluble in a variety of common solvents at room temperature, the crystallization of these materials cannot be induced by slow cooling. Suitable solution-crystallized specimens were obtained only by increasing the polymer concentration by extremely slow evaporation of the solvent (of the order of 1 week). The high solubility has to do with low values of melting temperature and heat of fusion for the E/P copolymers (extrapolated values for zero heating rate [25] are 37.2°C and 60.0°C for **HP15** and **HP21**, respectively). The thermal behavior will be the subject of a forthcoming publication [26].

The thickness of the solution-grown lamellae can be estimated from the length of the platinum shadow left behind an edge of a lamella. Lamella thicknesses between 10 and 20 nm with an error of measurement of about 30% were found. This value is precise enough to demonstrate that chain folding has taken place, remembering that the contour length of the polymers is between 140 nm (**HP15**) and 170 nm (**HP21**). On the other hand the observed lamellae are much too thick to be correlated to the sequence length of the methylene groups between methyl side groups.

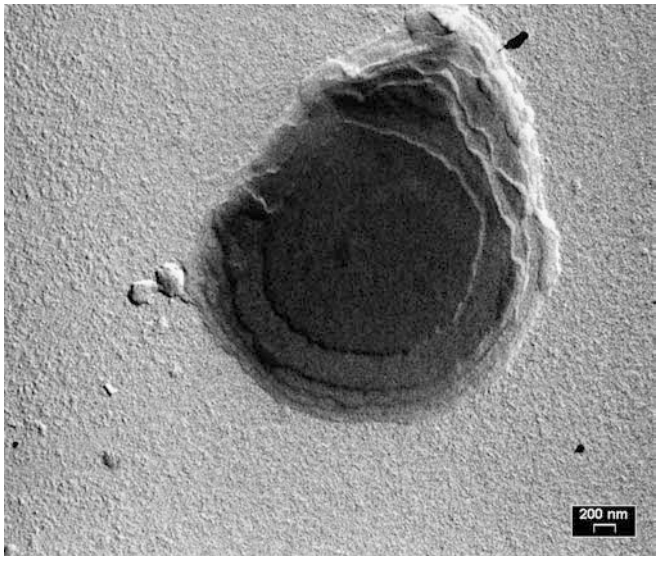

Fig. 1 Transmission electron micrograph of **HP21** crystallized from tetrachloroethylene solution

Lamellae are also the predominant morphological feature in the melt-crystallized E/P copolymers as illustrated in Fig. 2. This sample was prepared by pouring a solution of E/P copolymer in chloroform onto a water surface to obtain a thin film. This film was transferred onto a glass slide, heated above the melting temperature, and recrystallized by cooling to room temperature. SAXS of melt-crystallized bulk material gave only information on the presence of a long period (LP) when the material had been annealed extensively. Several orders of the LP reflection with the ratio of 1:2:3 where the basal reflection is not resolved also indicate lamellar morphology for the bulk material. The LP values compiled in Table 1 resulted from annealing the samples for 5 days.

Conformation and packing of ADMET E/P copolymer chains in the crystalline state

The following discussion is based mainly on powder diffraction data recorded by both a double-radius Debye and a Kiessig camera. Electron diffraction patterns augment the database.

The first striking observation is that wide-angle X-ray diffraction (WAXD) patterns of the homologues **HP15** and **HP21**, crystallized from the melt, differ significantly from each other and from the known pattern of orthorhombic linear PE or of random E/P copolymers. The relevant Debye powder patterns are displayed in Fig. 3. At higher resolution we have also recorded additional weak reflections from annealed samples of the E/P copolymers. These reflections have high d values and are

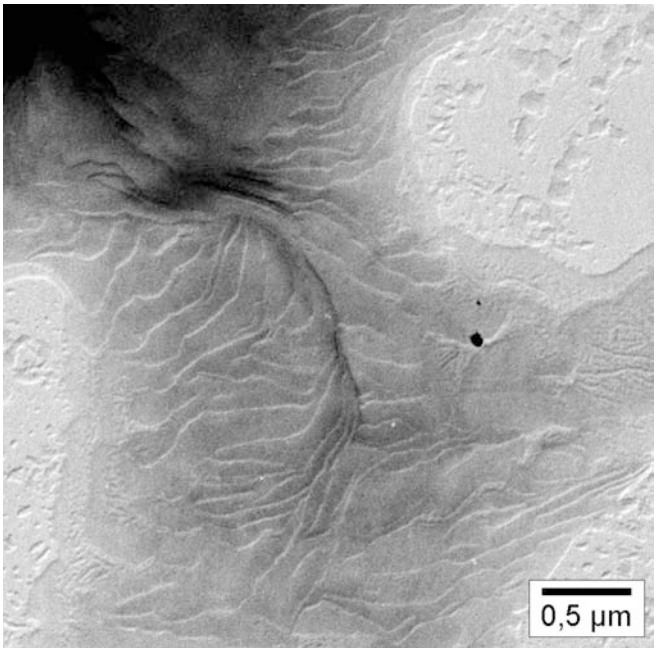

Fig. 2 Transmission electron micrograph of **HP21** recrystallized from the melt

Table 1 Point-collimated SAXS data for E/P copolymers[a]

Polymer	Order of reflection	d value (Å)
HP15	1st	197[b]
	2nd	99
	3rd	63
HP21	1st	164[b]
	2nd	82
	3rd	54

[a]**HP15** sample annealed at 20°C for 120 h; **HP21** sample annealed at 45°C for 120 h prior to measurement
[b]The d value of the 1st-order reflection is calculated from measured 2nd- and 3rd-order reflections

incompatible with a lattice the dimension of which is controlled by the chain repeat of linear PE (typically a subcell composed of two $-CH_2-CH_2-$ zigzag units). For random copolymers, pendant groups normally act as lattice defects that broaden the reflections, change their relative intensities, and shift the reflex positions with respect to linear PE. To the authors knowledge the additional reflections have never been previously observed for either linear or randomly (statistically) branched polyethylenes—a point that is worth noting in this case.

Electron diffraction data of ADMET E/P copolymers agree with X-ray data within the limits of error. The copolymers are extremely sensitive to beam damage; thus, the majority of data was attained at a temperature of −130°C to minimize sample degradation.

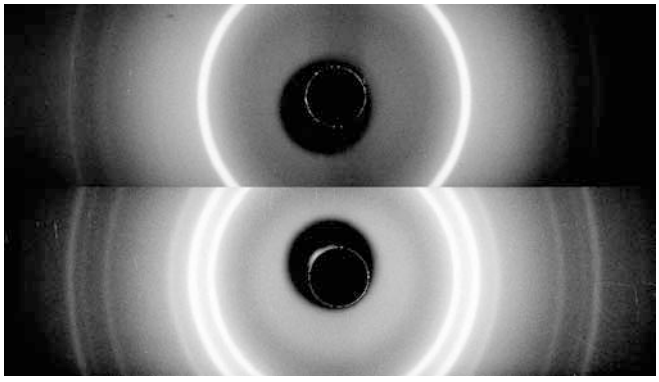

Fig. 3 Debye powder patterns of melt crystallized samples of **HP15** (*top*) and **HP21** (*bottom*)

Only electron diffraction data were acquired from solution-crystallized E/P copolymers. Electron diffraction patterns of polymer single crystals have in most cases the advantage that indexing is more straightforward because they show isolated point reflections. In the present case diffraction patterns like the one shown in Fig. 4 were the exception. When the crystal was appropriately tilted on the specimen stage the diffraction pattern exposed a sequence of reflections of consecutive zones that allows us to derive repeat distances along the polymer chain. This peculiarity is due to the fact that reflections of thin lamellae degenerate to spikes in reciprocal space. A circle in Fig. 4 labels such a superimposition of reflections of three zones. Unfortunately most of the solution-crystallized objects gave diffraction patterns composed of one or several rings, for which proper indexing is as much a challenge as for the powder patterns obtained in the WAXD experiments. The observed d values of the innermost reflection rings vary significantly not only between samples of the same polymer but also among different sites of one and the same object, and in general, they do not agree with strong X-ray reflections of the same copolymer crystallized from the melt. These observations point toward polymorphism as a complicating feature.

Chain packing of **HP15**

The electron diffraction pattern displayed in Fig. 4 can serve as a starting point for a first, intuitive access to the packing of the polyethylene chains having pendant methyl groups at uniform distance. The pattern was recorded from solution grown (tetrachloroethylene) **HP15**. The crystal was tilted so that the incoming beam made an angle of 36° with the normal of the lamella surface. The diffraction pattern is composed of several zones exhibiting reflections of consecutive Miller indices ℓ. The distance of the reflections tells us that the chain repeat amounts to 3 to 4 nm, which matches the distance

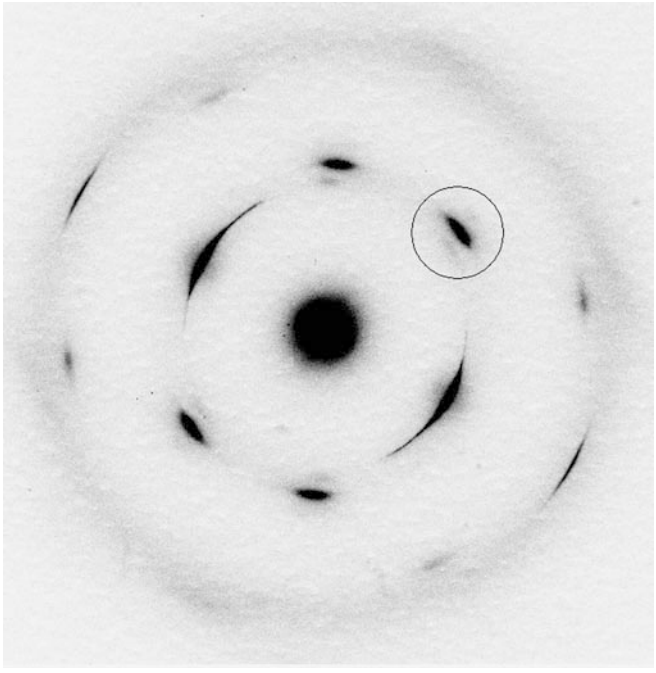

Fig. 4 Electron diffraction pattern of solution crystallized lamellae of **HP15** recorded at −130°C under a tilt angle of 36.5°

from the 1st to the 3rd side group along the chain. However, the substitution pattern along the chain is such that the configuration at the methyl branches is not stereoregular, and, moreover, we find an odd number of carbon atoms spanning the trajectory between adjacent methyl placements in every chain. Therefore, the unit cell parameter**c** should include at least 2 formula repeat units.

In most cases, the crystallites obtained from solution were so small that many individual and uncorrelated crystallites existed inside the selected area—even when a small aperture was chosen. Therefore, the electron diffraction pattern exhibits only continuous rings, as in WAXD powder patterns. In many cases only one single intense ring with a diameter corresponding to a d value > 4.5 Å occurred. Based on this observation one could suggest a hexagonal lattice.

Coming back to the pattern displayed in Fig. 4, the d value of the reflections (along the central line in NW–SO direction) that define the tilt axis is 4.58 Å. An indexing of 10.0 for a hexagonal lattice is unreasonable because then the calculated crystalline density of **HP15** would be much lower than the density of amorphous linear PE. In the light of the many and mostly very weak reflections seen in the X-ray powder pattern (not reproducible in the print of the Debye pattern in Fig. 3a) the lattice to which this ring belongs is most probably triclinic. A triclinic crystalline phase of linear PE has been discussed and was described by Turner–Jones [27]. A triclinic lattice enables better packing of the pendant groups because the methyl groups of adjacent chains can stagger and create less free volume. With this hypothesis in mind one can index the X-ray powder pattern. The refinement was started with the a and b parameters given by Turner–Jones for the triclinic unit cell; however, the c parameter was chosen in order to account for the 30 chain atoms as a possible crystallographic chain repeat. Starting the refinement with this parameter set, a unit cell was calculated, based on 20 observed reflections, with the following parameters:

$$a = 5.18\ \text{Å},\ b = 4.44\ \text{Å},\ c = 36.7\ \text{Å},\ \alpha = 89.7°,$$
$$\beta = 99.3°,\ \gamma = 113.9°.$$

From these lattice parameters a crystalline density (ρ) of 0.98 g cm^{-3} is calculated. The c parameter of the unit cell (36.7 Å) is substantially shorter than can be calculated for a pure *all-trans* chain of 30 methylene groups. The contour length would be 38.1 Å. Thus, the polymer chain must be distorted. It is not possible, however, to extract from the data whether the chain shortening is uniformly distributed or whether most of the zigzag units have the unchanged value of 2.54 Å. In the classically studied cases of branched polyethylenes made via chain propagation techniques, the chain shortening has been found to be more or less concentrated within a region of a few methylene groups adjacent to the methyl defects.

However, there exists undoubtedly a hexagonal sublattice of which the typical reflections of the basal plane are seen. The expected reflections 10.0, 11.0, 20.0, 21.0, and 22.0 can be indexed as a consistent set both in the X-ray powder pattern and in electron diffraction patterns, where the sequence of hk.0 reflections is unambiguously identified. The hexagonal lattice is obviously a sublattice of the triclinic unit cell in which linear segments between the methyl branches participate and not another crystalline modification adopted by the E/P copolymers. No solution-crystallized platelet exhibiting a hexagonal hk.0 diffraction pattern was found with its (fold) surface oriented normal to the incident beam. Electron diffraction patterns at oblique beam incidence with a ring corresponding to $d_{10.0} = 4.33$ Å corresponding to mutual chain distances of 5.00 Å point to a hexagonal basal net that is oriented normally to the chain stems. The plane of the hexagonal basal net is not coplanar to another plane containing the defects (methyl side groups) which is parallel to the **a**–**b** plane of the triclinic cell. In Table 2 an attempt is made to point out the superposition of the hexagonal basal net and the triclinic unit cell. We suggest that hexagonal hk. ℓ reflections with $\ell \neq 0$ do not appear because the conformation of the methylene groups between the branching points is not regular enough.

Hexagonal diffraction patterns containing the 10.0 reflection have also been observed when films were

prepared by pouring a chloroform solution onto a water surface. Corresponding d values varied between 4.37 Å and 4.23 Å. To explain the values at the lower limit, one has to take into account that most of the electron diffraction work was done at typically −130°C in order to minimize irradiation damage. Owing to this fact, this result is straightforward because we have invoked effects of thermal expansion/contraction on the cell parameters.

Not all of the reflections observed in the present work can be coherently explained at the current state of affairs. In particular reflections that appear only after heat treatment at low scattering angles are not seen in the electron diffraction diagrams of the [001] zone. From this observation one may conclude that they originate from the meridian of a hypothetical fiber diagram (i.e., are related to the *c*parameter of the unit cell). These data are compiled in Table 3. A possible interpretation will be given below.

Chain packing of **HP21**

The appearance of powder diffraction patterns of **HP21** is markedly different from those obtained for **HP15**. The strongest reflections occur at d values of 4.73 Å and 4.09 Å. The innermost reflections (rings) of electron diffraction patterns are positioned around 4.6 Å, 4.4 Å, or 4.3 Å.

Most of the reflections could again be indexed in terms of a unit cell close to the Turner–Jones cell for a sequence of 42 chain atoms. Refinement leads to the following unit cell parameters:

Table 3 Low-angle powder diffraction data for **HP15** recorded using a Kiessig camera

2ϑ (°)	d (Å)	Relative intensity
3.27	27.0	w
6.55	13.5	m
7.82	11.3	w
10.76	8.22	vw

$$a = 5.30\text{Å},\ b = 4.49\text{Å},\ c = 53.0\text{Å},\ \alpha = 91.2^\circ,$$
$$\beta = 102.9^\circ,\ \gamma = 113.0^\circ.$$

The crystalline density (ρ) is calculated to be 0.91 g cm^{-3}. Table 4 summarizes observed and calculated reflections. In addition, the reflections that fit to a plane hexagonal sublattice and may be indexed as hk.0 are indicated.

As in the case of **HP15**, thermal treatment gave rise to reflections at low angles, which cannot be interpreted in this scheme. The corresponding values are compiled in Table 5 and will be discussed elsewhere (vide infra).

Discussion

The first conclusion that can be unambiguously drawn from morphology and diffraction data and considering the molecular structure of the E/P copolymers is that a significant proportion of the methyl side groups become incorporated into the crystalline core of the material.

Table 2 Debye–Scherrer powder diffraction data for **HP15** and electron diffraction data belonging to the triclinic unit cell[a]

X-ray data 2ϑ (°)	d observed[b] (Å)	Triclinic *hkℓ*	Hexagonal *hk.ℓ*	Relative intensity	d calculated (Å)
14.8	*5.99*	006		vvw	6.03
18.0	*4.93*	?		vvw	
	4.60	100			4.66
19.4	*4.58*	100		vs	4.66
20.5	*4.33*	102	10 0	vs	4.34
	3.98	$\bar{1}10$			3.97
	3.89	104			3.86, 3.92
24.3	*3.66*	105		vvw	3.64
	3.58	014			3.61
	3.54	$1\bar{1}4$			3.53
25.8	*3.45*	$\bar{1}16$		vvw	3.45
27.2	*3.28*	$\bar{1}17$		vvw	3.28
29.3	*3.05*	$\bar{1}17$		vvw	3.05
34.7	*2.59*	110		m	2.59
35.8	*2.51*	$2\bar{1}1$	11.0	m	2.51
	2.48	$2\bar{1}1$			2.49
38.9	*2.32*	200		vvw	2.33
40.5	*2.23*	$1\bar{2}0$	20.0	m	2.22
49.9	*1.83*	$2\bar{2}6$		w	1.84
53.5	*1.71*	$\bar{3}10$	21.0	vvw	1.70
73.3	*1.29*	220		w	1.29
76.8	*1.24*	$4\bar{2}2$	22.0	w	1.24
79.5	*1.21*	0.0.30		vw	1.21

[a]Reflections belonging to the hexagonal basal net are labeled
[b]The measured data are the scattering angles. Corresponding d values in italic letters

Table 4 Scattering Data for **HP21** from X-ray powder patterns and electron diffraction, belonging to the triclinic unit cell[a]

X-ray data 2ϑ (°)	d observed[b] (Å)	Triclinic $hk\ell$°	Hexagonal $hk.\ell$	Relative intensity	d calculated (Å)
	26.8	002			25.7
	12.6	004			12.8
18.75	*4.73*	100		vs	4.72
	4.59	101			4.59
	4.42	102			4.45
	4.30	103	10.0		4.28
	4.16	104			4.11
21.75	*4.09*	010		vs	4.10
	3.95	01̄6			3.89
	3.74	106			3.75
25.1	*3.55*	016		s	3.54
	3.42	0.1̄.10			3.41
27.0	*3.30*	018		vvw	3.28
34.7	*2.59*	110		m	2.61
	2.50	2̄10			2.54
36.5	*2.46*	0.0.21		vw	2.44
	2.46	114	11.0		2.46
38.2	*2.36*	200		w	2.36
	2.29	21̄6			2.31
40.25	*2.24*	12̄0		s	2,24
	2.15	206	20.0		2.14
43.9	*2.06*	020		m	2.05
47.75	*1.91*	22̄6		vw	1.91
53.25	*1.72*	3̄10	21.0	w	1.72
61.25	*1.51*	304		vw	1.52
68.0	*1.38*	03̄6	22.0	vvw	1.38
74.75	*1.27*	42̄0		vw	1.27
78.25	*1.22*	0.0.42		vw	1.22

[a]Reflections belonging to the hexagonal basal net are labeled
[b]The d values in italic letters are calculated from the scattering angles measured in a Debye powder pattern

Table 5 Low-angle powder diffraction data for **HP21** recorded using a Kiessig camera

2ϑ (°)	d (Å)	Relative intensity
3.30	26.8[a]	vw
5.77	15.3	vvw
6.10	14.5	m
6.62	13.4	vvw
7.02	12.6[a]	m
7.41	11.9	vvw
8.94	9.89	vvw
9.78	9.04	vvw
9.93	8.91	w
11.34	7.80	w

[a]Reflections matching the triclinic lattice

The sequence length of the methylene groups does not determine the lamella thickness. The copolymer is, however, subject to chain folding. For the case of a linear C_{35}-alkane with a pendant chlorine residue in position 18, it has been shown that a fold is induced at the chlorine position [2]. Therefore, it may be justified to suggest that the position of a pendant methyl group is a favored place to initiate a fold. However, a considerable number of pendant groups of the same chain must remain in the interior of the crystallite; they act as packing defects within the lattice. The uniform distance between the defects of one and the same chain stem favors that they may be arranged in parallel planes in order to reduce the volume needed to adjust for the side groups. This necessity prevents that the side-group-containing planes are perpendicular to the chain stems. A triclinic lattice facilitates packing of the pendant groups inside a crystal by minimizing the spatial requirements via a mechanism involving the staggering and axial shifts of adjacent chains. Despite the non-stereoregular attachment of the methyl side groups we use the term ''unit cell'' for the smallest unit in the triclinic lattice. The non-stereoregular placement of the methyl groups exerts, in addition, a distortion of the chain segments between the branch positions (or parts thereof). This conformational distortion should be more pronounced when there are a relatively smaller number of methylene units between the branch points (**HP15** < **HP21**). Thereby, the chain stems are prevented from organizing in a pure *trans* conformation as a planar zigzag chain. The refinement of the *c* parameter results in a nearly pure *trans* sequence for **HP21** (53.04 Å instead of 53.34 Å for a sequence of 21 planar segments in zigzag geometry. This means a shortening of a zigzag unit of 0.56% with respect to the ideal *trans* conformation). In contrast, **HP15** exhibits 36.73 Å instead of 38.1 Å for a sequence of 15 planar segments. This translates into a shortening of 3.60%.

This result needs to be discussed in the context of an observation in the Raman spectra of both copolymers as is displayed in Fig. 5. In the C–C stretching region **HP15** displays a band at 1,084 cm^{-1} that is absent in the

spectrum of **HP21**. This rather broad feature has been previously observed at 1,080 cm^{-1} for linear PE by several authors and was unambiguously assigned to an amorphous-like packing region containing many *gauche* conformers. In fact, this spectral region was thought to originate from the sum of all deformations within the fold region [28, 29, 30]. In the current case the structural impact is certainly not only due to the folding, which is present in the crystals of both **HP21** and **HP15**, but will also be associated with the conformational constraints enforced by packing of the non-stereoregularly attached methyl groups into a lattice composed of $–CH_2–$ segments. Without question, sites of conformational irregularity will produce *gauche* (or *gauche*-like) conformers. This effect should be more prevalent when there are a smaller number of methylene groups between the branch points (i.e., the shorter the connecting methylene segments, the more opportunity there is for conformer disordering). The diffraction and microscopy results for **HP15** and **HP21** clearly indicate that the degree to which the conformational disordering affects the final morphology of the material is highly dependent on the distance between side groups.

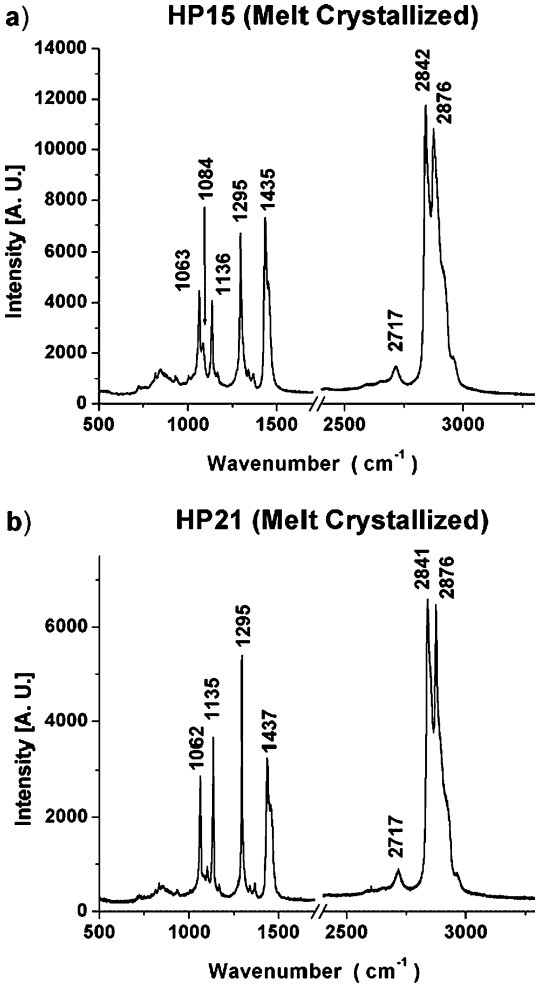

Fig. 5a,b Raman spectral data for **a HP15**, **b HP21**. Samples were crystallized from the melt and analyzed at room temperature

The geometry of the unit cells of both E/P copolymers is similar. The chain cross-sections are 20.7 $Å^2$ and 21.1 $Å^2$ for **HP15** and **HP21**, respectively. The crystalline densities, however, differ significantly with $\rho = 0.98$ g cm^{-3} for **HP15** and $\rho = 0.91$ g cm^{-3} for **HP21**. We attribute this discrepancy to the higher level of distortions found within the chains of **HP15**. It is worthwhile mentioning that the triclinic cell with its mode of chain packing matches closely the dense oblique chain packing in Kitaigorodsky's terminology T[$\pm 1/2$,1] with the layer cell $a = 5.2$ Å, $b = 4.3$ Å, and $\gamma = 109°$ (a and b interchanged with respect to the original denomination) [31].

The methylene segments between the branch points are almost hexagonally packed. However, the hexagonal subcell has to be reduced to a hexagonal basal net with the polymer chains being oriented normal to the net plane. This plane, however, is not the **a**–**b** plane of the triclinic cell on which the pendant groups are located. It seems that the reflections able to be assigned to a hexagonal basic net cannot be indexed for all samples or all thermal histories by the same reflections of the triclinic unit cell. Most likely these discrepancies are caused by some type of glide movement along the chains that originate from conformational changes not only in the fold planes. A comparison with data of linear PE crystallized under high pressure shows that hk.0 reflections of a hexagonal net are observed but reflections with $\ell \neq 0$ are not [32]. The main reason for this peculiarity is the occurrence of *gauche* sequences distributed along the *trans* chain. Yamamoto was able to calculate a model and concluded that there would have to be an accumulation of *gauche* sequences (approximately 5 methylene groups) in order to produce this result [33].

By the distribution of similar distortions along the E/P copolymer chain the orders of reflections characterizing the direction normal to the lamella surface could become incommensurate. Examples for such a possibility are known in the literature and have a number of different origins. The best-studied case is a random copolymer of 4-hydroxybenzoic acid and 6-hydroxy-2-naphthoic acid [34]. Other examples are α-keratin, drawn PE [35], and annealed bulk PE [36]. In polyamide, which also has a large chain repeat, incommensurate reflections are due to interplay between lattice and structure factor [37], because lamella thickness is limited to only a few chain repeats. In case of the ADMET E/P copolymers studied here, a similar scenario is at work; because as diffraction results have shown, the lamellae are only about 5 (**HP15**) and 3 (**HP21**) unit cell dimensions thick in the c direction.

Recently, Ze-sheng Li and coworkers published a molecular dynamics (MD) simulation study that examined a series of single copolymer chains containing

precisely controlled methyl branching. The methyl group was placed on every 9th, 13th, 15th, 21st, 51st, and 101st backbone carbon [38]. They found that as the defect content was decreased, the probability of *trans* segments increased—which without question is a prerequisite for the formation of a lamellar morphology. Deviations from the *trans* conformation were observed in this simulation, but the torsion angles were rather close to the *trans* and not the *gauche* conformation. The other finding, that the majority of methylene side groups should be located in the fold region at the lamella surfaces and therefore the lamellar thickness should be less than 5 nm, is not confirmed by our experimental result.

Conclusions

The experimental evidence obtained in this work has shown that a significant fraction of the methyl side groups becomes incorporated into the crystalline regions. However, as shown by diffraction experiments and Raman spectroscopy, the pendant methyl branches lead to both lattice defects and conformational disordering along the chain stems. This result helps to explain the strongly reduced melting points and heat of fusion previously found for these ADMET E/P copolymers during differential scanning calorimetry (DSC) measurements [26]. Further insights into the thermal behavior of these materials in regards to their packing ability will be presented in a forthcoming publication.

Acknowledgment Financial support by the National Science Foundation under grant Nr 98-06492, PI K.B.W., University of Florida, and by the Max Planck Research School on Polymer Materials Science is gratefully acknowledged.

References

1. Alamo RG, Mandelkern L (1994) Thermochim Acta 238:155
2. Gutzler F, Wegner G (1980) Colloid Polym Sci 258:776–786
3. Wunderlich B, Poland D (1963) J Polym Sci Part A Polym Chem 1:357–372(1)
4. Gerum W, Höhne GWH, Wilke W, Arnold M, Wegner T (1996) Macromol Chem Phys 197:1691–1712
5. Ungar G, Zheng X-b (2001) Chem Rev 101:4157–4188
6. Wunderlich B (1980) Macromolecular physics, vol 3. Academic Press, New York
7. Mandelkern L (1964) Crystallization of polymers. McGraw-Hill, New York
8. Sun Z, Yu F, Qi Y (1991) Polymer 32:1059-60
9. Simanke AG, Alamo RG, Galland GB, Mauler RS (2001) Macromolecules 34:6959–6971
10. Guerra G, Galimberti M, Piemontesi F, de Ballesteros OR (2002) J Am Chem Soc 124:1566-1567
11. Howard PR, Crist B (1989) J Polym Sci Part B Polym Phys 27:2269–2282
12. Vonk CG (1972) J Polym Sci Part C 38:429–435
13. Burfield DR, Kashiwa N (1985) Makromol Chem 186:2657–2662
14. Androsch R (1999) Polymer 40:2805–2812
15. Androsch R, Blackwell J, Chvalun SN, Wunderlich B (1999) Macromolecules 32:3755–3740.
16. Hu W, Srinivas S, Sirota EB (2002) Macromolecules 35:5013–5024.
17. Baker AME, Windle AH (2001) Polymer 42:651–655
18. Baker AME, Windle AH (2001) Polymer 42:667–680
19. Baker AME, Windle AH (2001) Polymer 42:681–698
20. Smith JA, Brzezinska KR, Valenti DJ, Wagener KB (2000) Macromolecules 33:3781–3794
21. Woodward AE (ed) (1988) Atlas of polymer morphology. Hanser, Munich
22. Hemsley DA (ed) (1989) Applied polymer light microscopy. Elsevier, New York
23. Sawyer LC, Grubb DT (1987) Polymer microscopy. Chapman and Hall, New York
24. Bassett DC (1981) Principles of polymer morphology. Cambridge University Press, Cambridge
25. Illers K-H (1974) Eur Polymer J 10:911–916
26. Smith JA, Wagener KB, Lieser G, Wegner G (2004) Thermal behavior of model ethylene/propylene copolymers with precise methyl branch placement (in preparation)
27. Turner-Jones A (1962) J Polym Sci 62:S53–S56
28. Lee K-S, Wegner G, Hsu SL (1987) Polymer 28:889–896
29. Tashiro K, Sasaki S, Kobayashi M (1996) Macromolecules 29:7460–7469
30. Strobl GR, Hagedorn W (1978) J Polym Sci Part B Polym Phys 16:1181–1193
31. Kitaigorodsky AI (1973) Molecular crystals and molecules. Academic Press, New York, chap 9
32. Bassett DC (1982) The crystallization of polyethylene at high pressures. In: Developments in crystalline polymers-1. DC Bassett Ed, pp 115–150
33. Yamamoto TJ (1979) Macromol Sci Phys B 16:487–509
34. Blackwell J, Gutierrez GA, Chivers RA (1984) Macromolecules 17:1219; Bonart RC, Blackwell J, Biswas A (1985) Makromol Chem Rapid Commun 6:353–359; Chivers RA, Blackwell J (1985) Polymer 26:997.
35. Bonart RC (1975) Prog Colloid Polym Sci 58:36–43; Bonart R (1966) Kolloid-Z u Z Polymere 211:14–33; Bonart R, Spei M (1972) Kolloid-Z u Z Polymere 250:385–393
36. Reinhold Ch, Fischer EW, Peterlin A (1964) J Appl Phys 35:71–74
37. Wallner LG (1948) Mh Chem 79:279–295
38. Zhang X-b, Ze-sheng L, Lu Z-y, Sun C-C (2002) Macromolecules 35:106–111